Nuclear levels and structure from the decays of ^{213}Bi and ^{209}Tl

G. Ardisson, V. Barci, and O. El Samad
Laboratoire de Radiochimie, Faculté des Sciences, Université de Nice, F-06108 Nice Cédex 2, France
(Received 26 June 1997)

Direct γ and γ-γ coincidence spectra of pure ^{209}Tl and ^{213}Bi sources obtained by radiochemical continuous separation were measured with coaxial and planar HPGe detectors. In ^{209}Tl the half-life was measured, the β-decay energies and intensities of 11 γ transitions were reported, and a new decay scheme was proposed. In ^{213}Bi β decay 22 transitions were observed, of which 18 were assigned to a new ^{213}Po level scheme accounting for 9 excited states. [S0556-2813(98)03402-5]

PACS number(s): 23.20.Lv, 21.60.Cs, 23.40.−s, 82.55.+e

I. INTRODUCTION

The knowledge of ^{213}Po nuclear structure would be interesting for the study of nucleon-nucleon interactions, since it has only two protons and three neutrons outside the doubly magic ^{208}Pb core. Moreover, the analytical superasymmetric fission model (ASFM) of Poenaru and Ivascu [1] predicts this nucleus to be the best candidate for ^{5}He emission. These authors calculated the process half-life against ^{213}Po excitation energy [1,2]. Besides the two close isotopes ^{212}Po and ^{214}Po own α-emitter excited states, so-called long-range α emitters. Very few experimental data were known about the ^{213}Po ($T_{1/2}$=4.2 μs) level scheme (see Ref. [3], and references therein), because it cannot be reached by nuclear reactions and its levels can only be fed by ^{213}Bi ($T_{1/2}$=45.6 min) β decay (97.91%). In the last decade this decay was extensively studied by measuring γ-decay spectra of the nuclide in equilibrium with the ^{229}Th parent and its daughters, through the decay chain $^{229}\mathrm{Th} \rightarrow {}^{225}\mathrm{Ac} \rightarrow {}^{221}\mathrm{Fr} \rightarrow {}^{217}\mathrm{At} \rightarrow {}^{213}\mathrm{Bi} \rightarrow {}^{213}\mathrm{Po}$, by Dickens and McConnell [4] and by Helmer *et al.* [5]. Owing to such a complexity the assignment of γ lines to transitions in a given nucleus was a hard task. Besides any ^{229}Th sample was contaminated by ^{228}Th, generating high-energy-γ emitter daughters. Therefore the decay was investigated using radiochemically separated ^{213}Bi sources to eliminate interferences due to parent nuclides [6]. But a further complication arises from the ^{213}Bi α-decay branch (2.09%) to the short-lived ^{209}Tl ($T_{1/2}$=2.2 min) with a poorly known γ spectrum. It feeds by β decay a 2152-keV level in ^{209}Pb, which deexcites by a strong cascade of 117, 465, and 1567-kev γ rays, generating high Compton background. So we decided to reinvestigate the ^{213}Bi decay using a pure source and to study the γ spectrum of the β decay of ^{209}Tl obtained by continuous radiochemical separation from its ^{213}Bi parent. The relevant scheme discussed in this paper is sketched in Fig. 1.

II. RADIOCHEMICAL SEPARATIONS AND EXPERIMENTAL METHODS

A. ^{213}Bi generator preparation

The ^{229}Th parent source was prepared from a 100-mg weight ^{233}U sample which has undergone no chemical treatment for 30 years. The uranium solution, in 10 M HCl, was loaded on a Dowex 1-X8 anion exchanger column and ^{229}Th in the eluate was evaporated to near dryness. The main impurity was ^{228}Th and its daughters generated by the α decay of ^{232}U, itself produced by $(n,2n)$ contamination reaction on ^{233}U, during reactor irradiation for source production. Thorium isotopes, in 8 M HNO_3, were fixed as nitrato complexes on a Dowex 1-8X column, while ^{224,225}Ra, ^{225}Ac and daughters passed through. After evaporation the eluate brought to 2 M in HNO_3, was percolated on a Dowex 50W-X8 column, thermostated at 80 °C, on which ^{225}Ac and daughters were fixed, washing with 2 M HCl allowed ^{213}Bi and ^{212}Pb to be discarded, then ^{225}Ra and ^{224}Ra were eluted with 3 M HNO_3; pure ^{225}Ac was eluted with 6 M HNO_3. ^{225}Ac was then loaded in 1 M HNO_3 on new Dowex 50W-X8 column used as a ^{213}Bi generator. ^{213}Bi sources, as anionic complexes, could be extracted every 2 h by washing the column with 0.5 M HCl; a small quantity of the short-lived ^{221}Fr ($T_{1/2}$=4.8 min) was also eluted.

B. ^{209}Tl source preparation and counting setup

^{213}Bi sources were loaded in 0.5 M HCl on a small column of Dowex 1-X8, fixed at the external wall of the lead castle shielding the HPGe detector and connected to a microcolumn of nickel hexacyanoferrate(II) (NiHCF), 0.10-g weight, placed in front of the detector. Washing with 2 cv (column volumes) of HCl discarded traces of ^{221}Fr remaining in the solution. The NiHCF exchanger was chosen to selectively fix the Tl^+ ion (radius r=147 pm), strongly retaining $^{221}Fr^+$ (r=180 pm) [7]. A 0.5 M HCl, 0.1 M thiourea

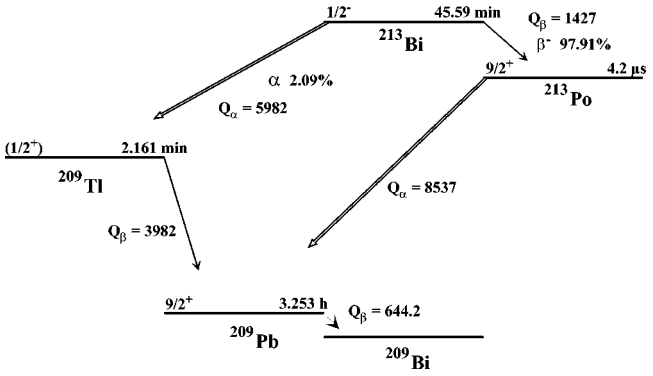

FIG. 1. Simplified decay scheme of ^{213}Bi. The Q values are in keV.

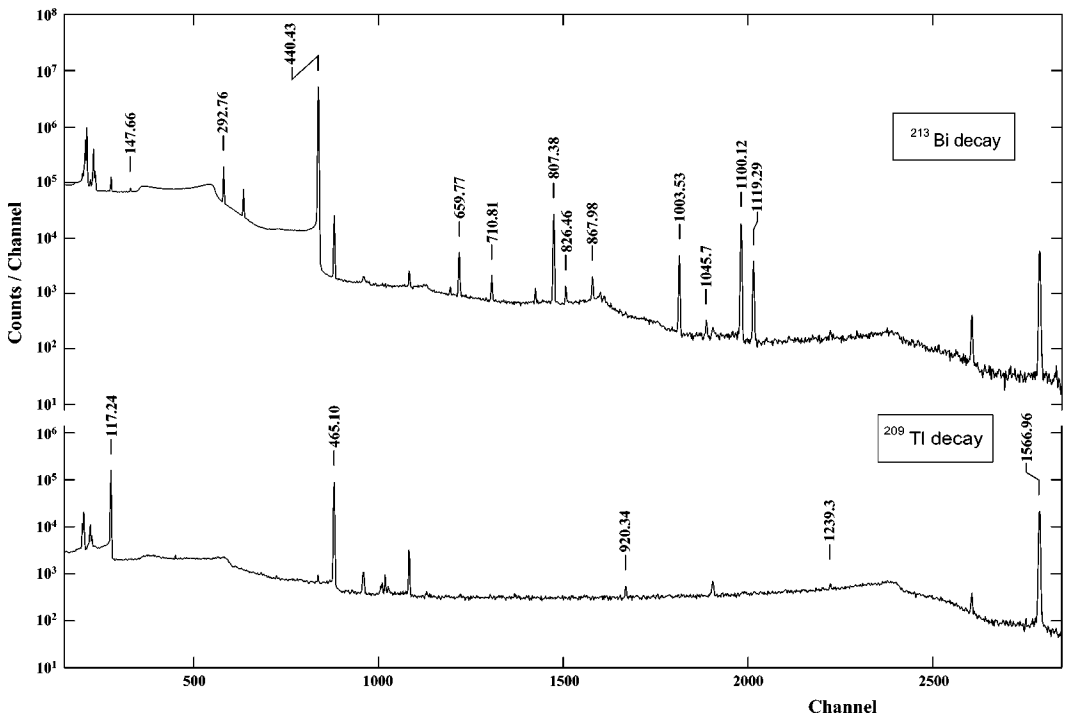

FIG. 2. Comparison of ^{213}Bi-decay and ^{209}Tl β-decay spetra. Only the main γ's are marked in the corresponding spectrum.

reducing solution was percolated through the column containing ^{213}Bi, using a microprocessor controlled peristaltic pump; in these conditions Bi remained on the column while Tl^+ passed through and was strongly fixed on the NiHCF column. At elution rate of 1.7 ml min^{-1} the continous fixation of ^{209}Tl on the column allowed a counting rate of 60 s^{-1} mainly depending on the weak ^{213}Bi α branching ratio $(2.09 \pm 0.03)\%$.

C. ^{213}Bi source preparation

Purified ^{213}Bi sources were measured by counting the Dowex 1-X8 column with continuous elution of $^{209}Tl^+$ using the reducing solution; however, thallium was not completely removed because the recoiling nuclei resulting from α decay might be implanted in the resin grains and could not be totally eluted. A decontamination factor of ^{209}Tl better than 350 was achieved with respect to the equilibrium mixture.

D. γ spectrometers

The spectrometers consisted of a n-type HPGe detector of 17% relative efficiency and energy resolution of 1.90 keV [full width at half maximum (FWHM) of the 1.33-MeV photopeak of ^{60}Co], and a 30% p-type coaxial HPGe detector with 1.90-keV resolution. We also used a 200-mm^2 area, 10-mm thick, planar HPGe detector for low-energy γ and x rays. Pulses were converted with an Ortec multichannel analyzer driven by a 486 PC computer. Spectrum files were transferred to a VAX 8530 computer and deconvoluted with the GAMANAL code [8]. The detectors were calibrated in energy and efficiency with standard ^{152}Eu and ^{207}Bi sources obtained from LMRI (Laboratoire de Métrologie des Rayonnements Ionisants).

III. MEASUREMENTS AND RESULTS

A. The ^{209}Tl decay γ spectrum

Sources of ^{209}Tl were counted with the 17 and 30% HPGe detectors; each γ spectrum was stored after 600-s counting time and afterwards summed in order to check the purity of the sources. 90 individual spectra were summed totalizing about 15 counting hours. In Fig. 2 we show a typical ^{209}Tl-decay γ-ray spectrum and Table I summarizes energy and intensity values obtained in this work. In addition to the main γ cascade 117-465-1567 keV, we observed 8 new weak γ lines; among them the 920.34 and 1239.76-keV γ transitions were also found in the ^{213}Bi-^{209}Tl mixture equilibrium decays [6].

TABLE I. γ transitions from ^{209}Tl β decay. Uncertanties are given in parentheses on the last digits of the figure.

E_γ (keV)	I_γ[a] (%)	E(level)[b] (keV)
117.24(5)	73(4)	2149.29
284.04(23)	0.14(7)	2315.67
311.5(3)	0.028(14)	2460.8
375.5(2)	0.070(15)	2524.79
465.10(5)	95(5)	2032.05
469.7(3)[c]	0.03(2)	
748.0(3)	0.09(3)	2315.67
920.34(9)	0.70(7)	3069.63
1239.76(15)	0.31(12)	3389.05
1329.3(3)	0.026(5)	3341.4
1566.96(5)	100(5)	1566.97

[a]For 100 total decay of the parent.
[b]Decaying level.
[c]γ not placed.

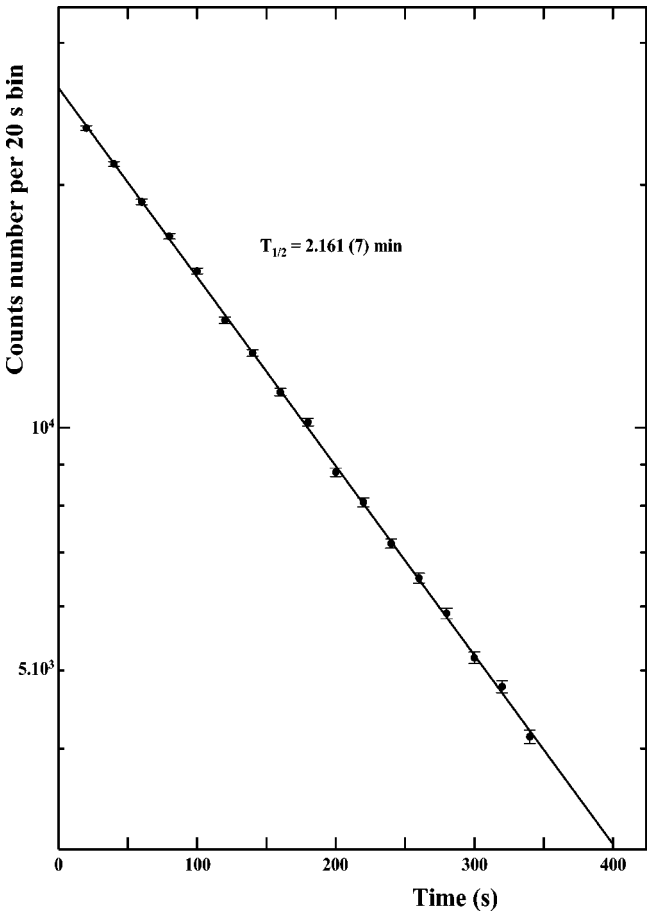

FIG. 3. Decay rate of ^{209}Tl.

B. ^{209}Tl half-life measurement

Since only one measurement of the ^{209}Tl half-life, by means of a GM counter and thallium purified sources, was published in 1950 [9], we decided to carry out a new measument using a multichannel anlyzer in multiscaling mode. ^{209}Tl sources were fixed on NiHCF columns 20 min each and the decay was followed over 400 s in 20-s bins. Twenty spectra were added and the experimental points were fitted using standard least square methods. The decay rate is plotted in Fig. 3. Our accurate value, $T_{1/2}=(2.161\pm0.007)$ min agrees well, within one stardard deviation, with Hagemann's [9,10] reported value $T_{1/2}=(2.20\pm0.07)$ min.

C. The ^{213}Bi decay γ spectrum

Twenty-eight ^{213}Bi sources were prepared and counted with continuous elimination of the ^{209}Tl daughter; the intensity ratio between the main photopeaks of 440 keV (^{213}Bi decay) and 465 kev (^{209}Tl decay) was measured in each run to check the decontamination factor with respect to the elution rate. 94 individual spectra were added to a total of 49-h counting. A typical γ spectrum is also show in Fig. 2, and Table II summarizes the results obtained in this work.

The γ line of 323.69 keV was assigned to the transition from the ^{209}Tl first excited $(3/2^+)$ to ground state $(1/2^+)$, from the α branch $(2.09\pm0.03)\%$ of the ^{213}Bi decay. The total transition intensity I_T may vary between 0.16 and 0.20 % depending upon the assumed multipolarity $[\alpha(E2)=0.0896,\ \alpha(M1)=0.331]$. If $E2$ then $I_T=(0.16\pm0.02)\%$, in good agreement with the intensity $(0.16\pm0.03)\%$ of the 5.549-MeV α group [11].

The 778.8-keV γ line (Table II) is interpreted as deexciting the ^{209}Pb first excited state $(I^\pi=11/2^-)$ through ^{213}Po $\rightarrow$ ^{209}Pb α decay. Its total transition intensity, (0.0043

TABLE II. γ transitions from ^{213}Bi β decay. Uncertanties are given in parentheses on the last digits of the figure.

E_γ (keV)	I_γ[a] (%)	E(level)[b] (keV)	E_γ (keV)	I_γ[a] (%)	E(level)[b] (keV)
147.66(5)	0.0148(12)	440.42	807.38(5)	0.241(15)	1100.16
292.76(5)	0.416(23)	292.77	826.47(6)	0.0057(5)	1129.27
323.69(5)	0.148(12)	[c]	867.98(3)	0.0111(11)	867.98
402.8(3)	0.00010(3)	1003.55	880.2(3)[e]	0.0029(10)	
440.43(5)	26.1(3)[d]	440.42	884.6(3)[e]	0.00029(10)	
574.8(3)	0.00063(17)	867.98	886.66(14)	0.00102(19)	1328.2[g]
600.7(3)	0.00070(22)	600.73	897.0(3)[e]	0.00031(9)	
604.9(3)	0.00050(18)	1045.67	1003.55(5)	0.050(5)	1003.55
646.03(9)[e]	0.00231(22)		1045.70(9)	0.018(3)	1045.67
659.77(5)	0.0361(20)	1100.16	1100.12(5)	0.259(16)	1100.16
710.81(21)	0.0102(11)	1003.55	1119.29(5)	0.050(3)	1119.27
778.87(5)	0.0043(4)	[f]	1328.2(3)	0.00039(14)	1328.2

[a]For 100 total decays $(\alpha+\beta^-)$ of the parent.
[b]Decaying level.
[c]To ^{209}Tl first excited to ground state transition from ^{213}Bi$\rightarrow$ ^{209}Tl α decay.
[d]Normalization value from Ref. [5].
[e]γ not placed.
[f]To ^{209}Pb first excited to ground state transition from ^{213}Po$\rightarrow$ ^{209}Pb α decay.
[g]The placement is uncertain.

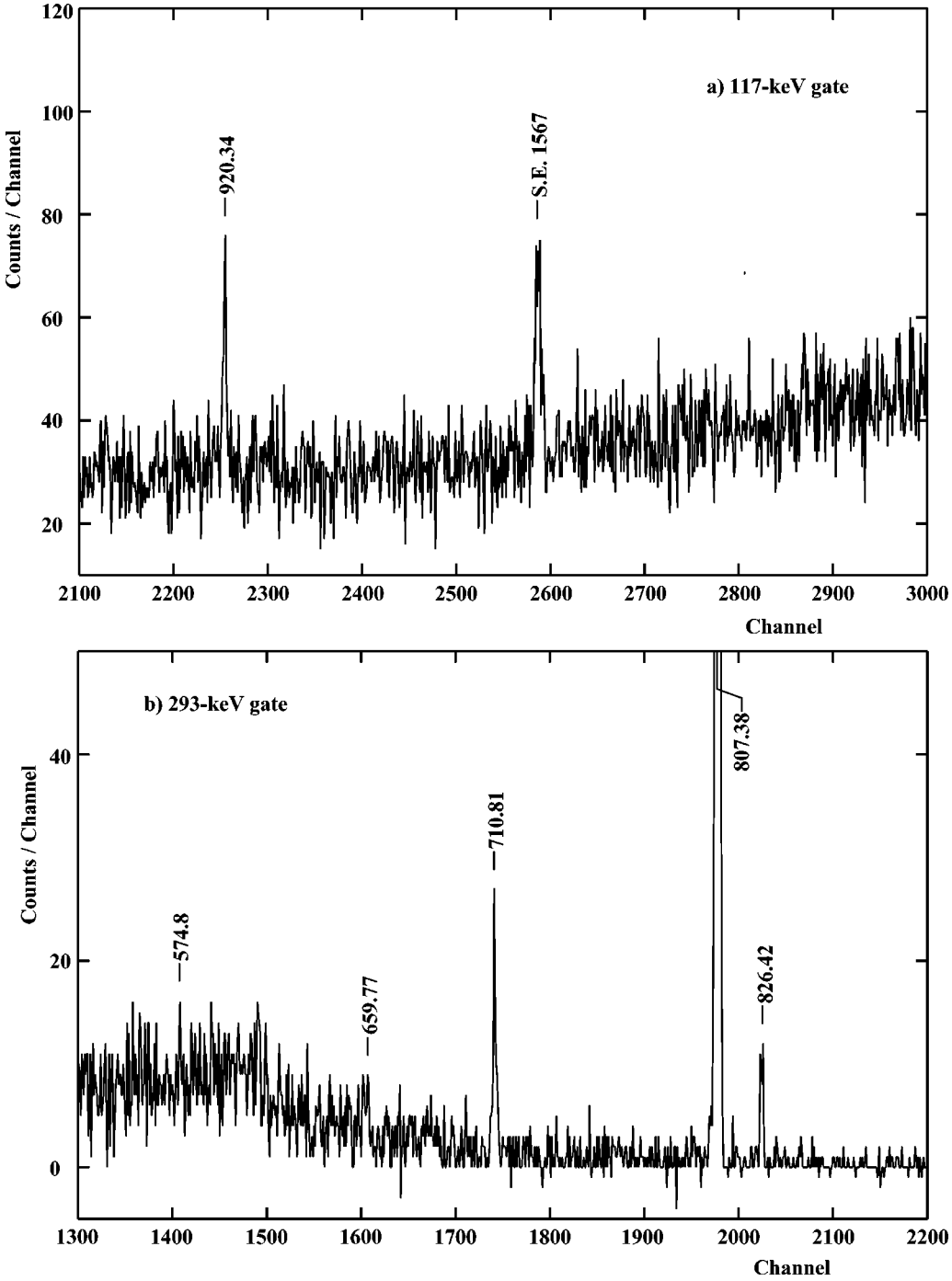

FIG. 4. Selected portions of coincidence spectra. (a) 117-keV gate in ^{209}Tl β decay. S.E. is the single-escape peak. (b) 293-keV gate in ^{213}Bi decay.

$\pm 0.0004)$%, agrees well with $I_\alpha=(0.006\pm 0.002)$% measured for the 7.612-MeV α group by Liang [12] or with $I_\alpha=(0.003\pm 0.001)$% for $E_\alpha=(7614\pm 10)$ MeV by Valli [13].

The 867.98-kev γ line, previously interpreted [6] as deexciting a ^{209}Tl state of the same energy is assigned here to ^{213}Po (Table I) as discussed in Sec. IV B 1.

D. γ-γ coincidence measurements

In order to assign γ lines to both ^{209}Pb and ^{213}Po level schemes γ-γ coincidence experiments were carried out using the long-lived ^{225}Ac parent in equilibrium with its daughters. The experimental setup included three n-type HPGe detectors of 20% relative efficiency and one 20-cm^2 planar HPGe detector. The acquisition system was described elsewhere [7]. Figure 4 shows typical gated spectra and Table III summarize the γ-γ coincidence data.

IV. DISCUSSION

A. The ^{209}Tl β-decay scheme

The ^{209}Pb level scheme as fed by the ^{209}Tl β decay, reported in Fig. 5, was build using γ-γ coincidence data and Ritz's combination principle. We also compared our data

TABLE III. γ-γ coincidence data.

β decay	Gate energy (keV)	Coincidence γ's[a]
^{209}Tl	117	311.5, 375.5, 465.1, 920.3, 1239.8, 1567.0
	376	117.2, 465.1
	465	117.2, 284.0, 1329.3, 1567.0
	920	117.2, 465.1, 1567.0
	1240	117.2, 465.1
	1329	465.1
	1567	117.2, 465.1, 748.0, 920.3, 1239.8, 1329.3
^{213}Bi	148	659.8
	293	147.7, 574.8, 710.8, 807.4, 826.5
	440	604.9, 659.8
	660	147.7, 440.4
	807	292.8

[a]Only transitions experimentally observed in direct coincidence with the corresponding gate are reported.

with nuclear levels observed in one-particle transfer reactions ^{208}Pb(d,p) [14], ^{208}Pb$(d,p\gamma)$ [15], ^{208}Pb(t,d) [16], ^{208}Pb$(\alpha,{}^3\mathrm{He})$ [17], ^{210}Pb(p,d) [18], and in the two-particle transfer reaction ^{207}Pb(t,p) [19]. Intensity balances at each level were calculated, correcting γ intensities for internal conversion, assuming pure multipolarities for the transitions

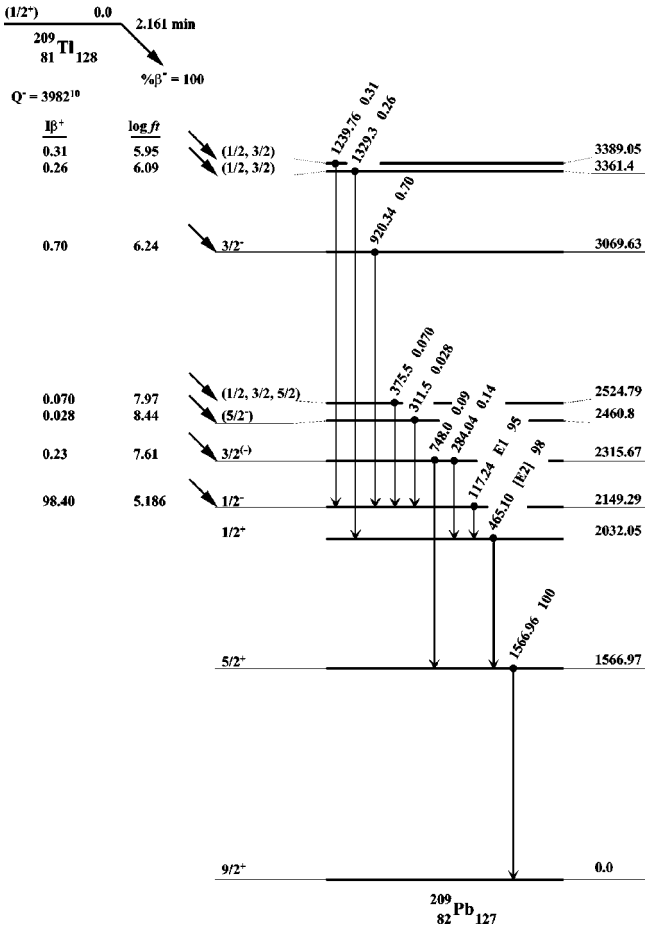

FIG. 5. ^{209}Tl β-decay scheme. Dots mark coincidence relations. Total intensities are per 100 decay of the parent. Energies are in keV. Square brackets around values means deduced from level scheme.

117.24 keV ($E1$), 465.10 keV ($E2$), and 1566.96 keV ($E2$). The leading intensity of the branch to the 2149-keV level was constrained by the condition $\Sigma I_\beta = 100$. Log ft values of β branches were computed from our measured half-life (Sec. III B), the β-decay energy $Q_{\beta^-} = (3982 \pm 10)$ keV [20], and the f_0 matrix elements by Gove and Martin [21].

Although no direct measurement of the ^{209}Tl ground-state spin had ever been made, the shell model allows to predict a $[(\pi 3s_{1/2})^{-1}(\nu 2g_{9/2})^2_{0^+}]$ two-paired-particle one-hole lowest configuration, so the state must be $I^\pi = 1/2^+$. The assignment is also supported by the $I = 1/2$ value measured for all the ground states of odd-mass thallium isotopes between $A = 199$ and 205. Hence β selection rules restrict direct feeding of ^{209}Pb levels to $I^\pi = 1/2^\pm$, $3/2^\pm$, and $5/2^-$ [22,23].

The levels at (1566.97 ± 0.05), (2032.05 ± 0.07), and (2149.29 ± 0.09) keV are known and will not be discussed.

1. Level at (2315.67± 0.20) keV

The feeding of a level at (2315.67 ± 0.20) keV in ^{209}Pb is proposed owing to the good agreement of sum relationship of the new weak γ transitions of 748.0 and 284.04 keV from this level to $I^\pi = 1/2^+$ and $5/2^+$ lower levels, observed in γ-γ coincidences, respectively, in 1567- and 465-keV gates. This level might be identified with the (2319 ± 2) keV level observed in ^{208}Pb(d,p) [14], ^{208}Pb$(d,p\gamma)$ [15], and ^{210}Pb(p,d) [18] reactions with probable spin $I^\pi = 3/2^{(-)}$. The corresponding β transition has log $ft = 7.6$, in agreement with the expected value for a $\Delta I = 0, \pm 1$ $(\Delta l = 1)$ $\Delta\pi$ yes, first-forbidden β transition [22,23], assuming a relative strong component of the $[(\nu 2g_{9/2})^2_{0^+}(\nu 3p_{3/2})^{-1}]$ configuration.

2. Levels at (2460.8± 0.4) and (2524.79± 0.22) keV

Two new levels are proposed at (2460.8 ± 0.4) keV and (2524.79 ± 0.22) keV to account for coincidences of 311.5- and 375.5-keV transitions observed in the 117-keV gate. The former might be identified with the (2463 ± 3)-keV level observed in ^{208}Pb(d,p) [14] and ^{210}Pb(p,d) [18] reactions with probable spin and parity $I^\pi = 5/2^-, 7/2^-$. The high

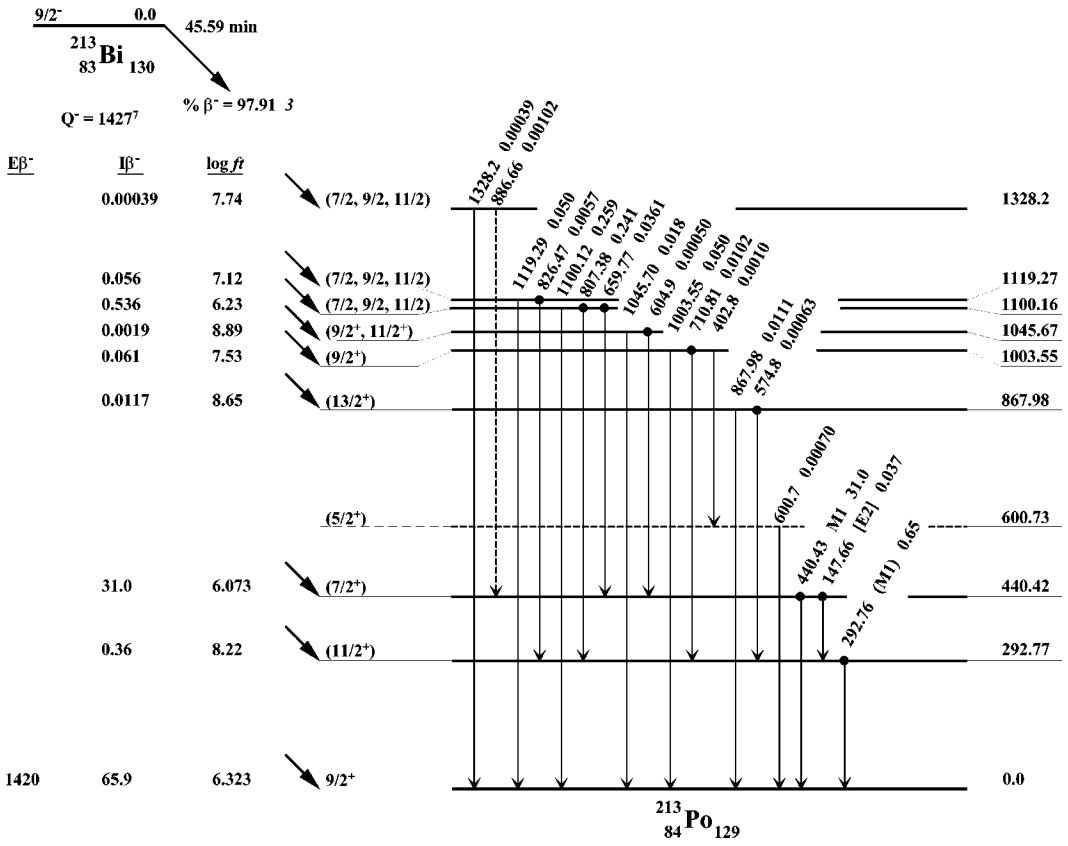

FIG. 6. Same as Fig. 5 for ^{213}Bi β decay.

log ft=8.4 value favors $I^{\pi}=5/2^{-}$ with a strong mixing of the $[(\nu 2g_{9/2})^{2}_{0^+}(\nu 2f_{5/2})^{-1}]$ configuration.

3. Level at (3069.63±0.13) keV

A level at (3069.63±0.13) keV is deduced from the coincidence of the 920.34-keV γ transition observed in the 117-keV gate. The level may be the (3076±5)-keV state ($I^{\pi}=3/2^{-}$) measured in the ^{208}Pb(d,p) [14] and ^{207}Pb(t,p) [19] reactions.

4. Level at (3361.4±0.3) keV

A level at (3361.4±0.3) keV is suggested on the basis of a γ transition of 1329.3 keV, seen in the 465-keV gate, decaying to the 2032.06-keV level ($I^{\pi}=1/2^{+}$). Its energy is in good agreement with the level (3361±3) keV measured in the ^{208}Pb(d,p) [14] reaction, but its decay mode disagrees with their assignment $I^{\pi}=(5/2^{-})$, since the $M2$ transition strenght would be out of limits. Therefore the identification with this level may be doubtful and a spin $I^{\pi}=(1/2,3/2)$ is more probable for log ft=6.1.

5. Level at (3389.05±0.18) keV

The (3389.05±0.18)-keV level is supported by the existence of a coincidence of the 1239.8-keV γ in the 117-keV gate. It may be identified with the (3387±4)-keV level observed in the ^{208}Pb(d,p) [14] and ^{207}Pd(t,p) [19] reactions. It may be assigned a spin $I^{\pi}=(1/2,3/2)$ for the low log ft=6.0 (Fig. 5).

B. The ^{213}Bi β-decay scheme

^{213}Bi deexcites mainly (97.91%) by β decay to ^{213}Po and by a weak α branch (2.09%) to ^{209}Tl. The most of γ transitions reported in Table II were assigned to the level scheme according to γ-γ coincidence data. Total transition intensities were calculated applying corrections for internal conversion, assuming $M1$pure multipolarities for the most intense 293- and 440-keV γ transitions, as measured in conversion electron experiment in previous works [3], and $E2$ multipolarity for the 148-keV transition according to level scheme as suggested by theoretical calculations (see Sec. IV C). Intensities were normalized to 100 total decays of the parent assuming an intensity (26.1±0.3)% for the 440-keV transition, as measured by Helmer *et al.* [5] with respect to 100 decay of the ^{229}Th parent. The β decay Q value was taken as (1427 ±7) keV [20]. The suggested decay scheme is shown in Fig. 6.

The spin of the ^{213}Bi parent ground state may be assumed $I^{\pi}=9/2^{-}$ as suggested by the extreme single-particle shell model. The lowest configuration of the unpaired proton outside the closed magic $A=208$ core is $[(\pi 1h_{9/2})(\nu 2g_{9/2})^{4}_{0^+})]_{9/2^-}$. Similarly the lowest configuration for the unpaired neutron in the ^{213}Po ground state is $[(\pi 1h_{9/2})^{2}_{0^+}(\nu 2g_{9/2})^{3}_{9/2^+}]_{9/2^+}$. The ground-state to ground-state β transition $(\nu 2g_{9/2})\rightarrow(\pi 1h_{9/2})$ will be first forbidden with $\Delta I=0$ $(\Delta l=1)$ and $\Delta\pi$.

1. Level at (867.98±0.03) keV

A (867.98±0.03)-keV level is proposed to account for the γ line of 867.98 keV and the coincidence of the 574- and

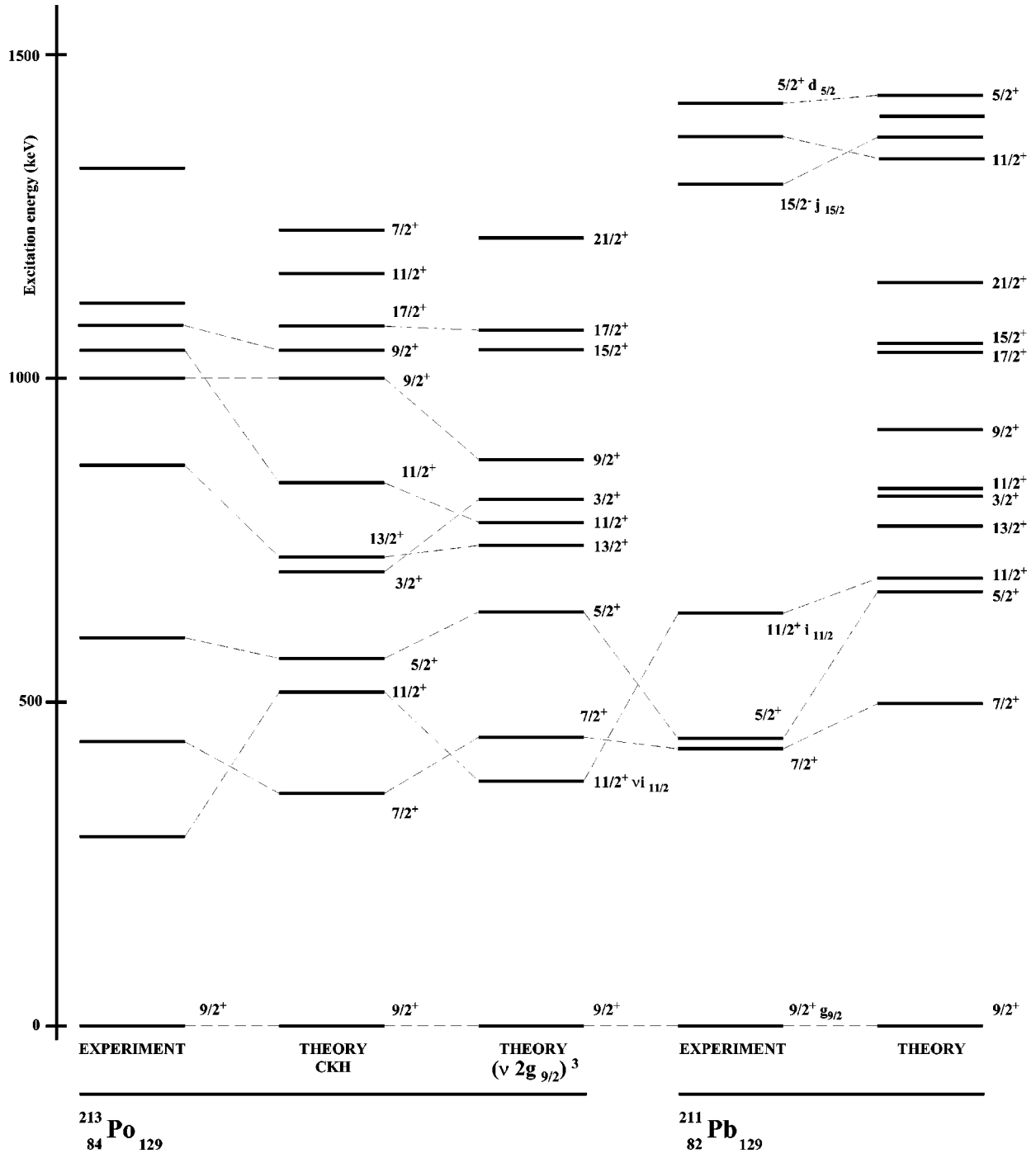

FIG. 7. Experimental and calculated level schemes of the ν^3 configuration. Dotted lines connect levels of similar structure and indicate possible identifications in the experimental scheme of ^{213}Po.

293-keV γ's. Previously this transition was erroneously assigned to the ^{209}Tl level scheme from the α branch of the decay [6]. This would imply a hindrance factor of about one unit caracteritic of a favored α transition, and therefore a spin assignment for the level inconsistent with the expected single-particle state in ^{209}Tl [24].

2. Level at (1003.55±0.05) keV

The (1003.55±0.05)-keV level, proposed in Ref. [6], was confirmed here by the presence of the 710-keV transition in coincidence with the 293-keV gating γ. A tentative level at (600.7±0.3) keV was proposed on the basis of sum relationship between the weak 600.7- and 402.8-keV γ transitions as cascading from the 1003.5-keV level (the order of the transitions may also be reversed).

3. Level at (1045.67±0.09) keV

A new level of (1045.67±0.09) keV was deduced from the coincidence of the 604.9-keV transition with the 440-keV gating γ and the existence of the 1046-keV γ transition.

TABLE IV. Experimental single-particle and two-particle energies outside the doubly magic ^{208}Pb core used in the calculation.

Single-particle configuration		e_j(keV)	E_j (keV)
$(\pi 1h_{9/2})$		0.0[a]	−3798.9(10)
$(\pi 2f_{7/2})$		896.29(5)[a]	−2903
$(\nu 2g_{9/2})$		0.0[b]	−3936.8(14)
$(\nu 1i_{11/2})$		778.8(3)[b]	−3158
Two-particle configuration	J^π	e_J (keV)	Δ_J (keV)
$(\pi 1h_{9/2})^2 J$	0^+	0.0[c]	−1185
	2^+	1181.40(2) [c]	−3
$(\nu 2g_{9/2})^2 J$	0^+	0.0[d]	−1249
	2^+	799.7(1)[d]	−450
	4^+	1097.7(10) [d]	−152
	6^+	1195.6(10) [d]	−54
	8^+	1279(30) [d]	30
$[(\nu 2g_{9/2})(\nu 1h_{11/2})]J$	(10^+)	1799(15) [d]	−229

[a]From ^{209}Bi [24].
[b]From ^{209}Pb [24].
[c]From ^{210}Po [26].
[d]From ^{210}Pb [26].

4. Level at (1100.16±0.04) keV

The (1100.16±0.04)-keV level, already suggested in Ref. [6], was confirmed on the basis of three γ transitions deexciting the state to the ground state and the two first excited levels, and from coincidence relationships with the 293- and 440-keV gating transitions (Table III). The 807-keV γ line, previously assigned to a level of the same energy, was observed in coincidence with the 293-keV gate.

5. Level at (1119.27±0.04) keV

A (1119.27±0.04)-keV level, previously proposed in Ref. [6], was confirmed on the basis of coincidence data (Table III).

6. Level at (1328.2±0.3) keV

A (1328.2±0.3)-keV level was proposed to account for a transition of the same energy.

C. Semiempirical shell-model energy calculations in ^{213}Po

Theoretical caculations were performed in the framework of the shell model, for a $(\pi^2\nu^3)$ configuration. The Hamiltonian was chosen as

$$H=\sum_i H_i+\sum_{i>k} H_{ik}, \tag{1}$$

with only one-particle and two-particle effective interactions. Taking eigenstates we get

$$E_J^*=\langle\Phi_J|H|\Phi_J\rangle=\left\langle\Phi_J\left|\sum_i H_i\right|\Phi_J\right\rangle+\left\langle\Phi_J\left|\sum_{i>k} H_{ik}\right|\Phi_J\right\rangle$$
$$=\sum_i \epsilon_i+\sum_{i>k}\Delta_J(ik)=\sum_{i=1}^{5} E_i+\sum_{i>k=1}^{5}\Delta_J(ik)-E_g, \tag{2}$$

where

$$|\Phi_J\rangle=|j_1{}^{n_1}(v_1J_1)j_2^{n_2}(v_2J_2)J\rangle$$

is the type of shell-model basis involved, of only two coupled shells with seniority, in the notation of De Shalit and Talmi [25]:

$$\epsilon_i=\langle\Phi_J|H_i|\Phi_J\rangle \quad \text{and} \quad \Delta_J(ik)=\langle\Phi_J|H_{ik}|\Phi_J\rangle$$

are single-particle and two-particle matrix elements; and

$$E_i=e_i-S_i$$

is the single-particle effective excitation energy relative to the ^{208}Pb inert core, experimentally taken from the level energy e_i and the particle separation energy S_i in the one-nucleon-plus-core close nuclei ^{209}Bi(π) and ^{209}Pb (ν) [24]:

$$E_g=\mathcal{B}(^{213}\text{Po})-\mathcal{B}(^{208}\text{Pb})$$

is the binding energy relative to the ^{208}Pb core. For the choice of the two configuration we note that the lowest experimental single-particle state energies relative to the core, at less than 1 MeV, are the $(\nu 2g_{9/2})$, $(\pi 1h_{9/2})$, and $(\nu 1i_{11/2})$ configurations (Table IV). In addition, the $(\pi^2\nu^3)$ ^{213}Po ground state configuration is most probably in the $[(\pi 1h_{9/2})^2 v=0 \;\; J=0^+]$ proton and the broken-pair configuration, $[(\pi 1h_{9/2})^2 22^+]$ is more than 1 MeV higher

(Table IV), so we can neglect it in this approximation. Finally we only retain the ν^3 configurations

$$[(\nu 2g_{9/2})^3 v J^+],$$

where $(v=1,\ J=9/2^+)$ or $(v=3,\ J=3/2^+\cdots 21/2^+)$, and

$$[(\nu 2g_{9/2})^2_{0^+})(\nu 1i_{11/2})]11/2^+$$

which from the preceeding discussion might adequately describe the lowest energy levels, below 1 MeV, in ^{213}Po. From a standard expansion of matrix elements between ν^3 configurations as a function of two-particle configuration matrix elements, using coefficients of fractional parentages (CFP) [25], the only extra experimental data needed are the two-neutron excitation energies e_J from the ^{210}Pb(ν^2) level scheme, which enter in the coupling energies

$$\Delta[(\nu 2g_{9/2})^2 J] = -S_{2n}(^{210}\mathrm{Pb}) + e_J(^{210}\mathrm{Pb}) - 2E(\nu 2g_{9/2}),$$

$(J^\pi = 0^+, 2^+, 4^+, 6^+, 8^+)$, and

$$\Delta[(\nu 2g_{9/2})(\nu 1i_{11/2})_J] = -S_{2n}(^{210}\mathrm{Pb}) + e_J(^{210}\mathrm{Pb}) - E(\nu 2g_{9/2}) - E(\nu 1i_{11/2}),$$

$(J^\pi = 1^+\cdots 10^+)$, where S_{2n} is the two-neutron separation energy. All the former $(\nu 2g_{9/2})^2$ states are known [26,27] and for the latter a probable (10^+) state was identified in ^{210}Pb (see Table IV). Taking these values, the level scheme, reported in Fig. 7, was calculated and compared with the experimental one, as a guide for parity and spins assignments. In the figure we we also reported the results (CKH) of Caurier [28] who performed a more extensive analysis in the complete particle-hole space around the ^{208}Pb core, with Kuo-Herling [29] residual interaction matrix elements. We also reported the experimental [30] and theoretical [31] data about the ^{211}Pb nucleus, which may also be described by a pure ν^3 configuration. The agreement between theory and experiment is quite good with the suggested identifications in the complete shell-model space as well as in the truncated one.

ACKNOWLEDGMENTS

We would like to thank C. Sauvage for kind permission to use the γ-γ spectroscopy device of the Center de Spectroscopie Nucléaire et de Spectroscopie de Masse (CSNSM) in Orsay.

[1] D. N. Poenaru and M. Ivascu, J. Phys. (Paris) **45**, 1099 (1984).
[2] D. N. Poenaru and M. Ivascu, Central Institute of Physics, Report No. NP27, Bucharest, 1983.
[3] Y. A. Akovali, Nucl. Data Sheets **66**, 237 (1992).
[4] J. K. Dickens and J. W. McConnell, Radiochem. Radioanal. Lett. **47**, 331 (1981).
[5] R. G. Helmer, C. W. Reich, M. A. Lee, and I. Ahmad, Int. J. Appl. Radiat. Isot. **37**, 139 (1986).
[6] M. C. Kouassi, A. Hachem, C. Ardisson, and G. Ardisson, Nucl. Instrum. Methods Phys. Res. A **280**, 424 (1989).
[7] A. Abdul-Hadi, V. Barci, B. Weiss, H. Maria, G. Ardisson, M. Hussonnois, and O. Constantinescu, Phys. Rev. C **47**, 94 (1993).
[8] R. Gunnink and J. B. Niday, Lawrence Livermore National Laboratory, Report No. UCRL-51061, 1972.
[9] F. Hagemann, Phys. Rev. **79**, 534 (1950).
[10] F. Hagemann, L. I. Katzin, M. D. Studier, G. T. Seaborg, and A. Ghiorso, Phys. Rev. **79**, 435 (1950).
[11] C. Graeffe, K. Valli, and J. Aaltonen, Ann. Acad. Sci. Fenn., Ser A VI, 145 (1964).
[12] C. F. Liang, thesis, Paris-Orsay University, 1969.
[13] K. Valli, Ann. Acad. Sci. Fenn., Ser A VI, 165 (1964).
[14] D. G. Kovar, N. Stein, and C. K. Bockelman, Nucl. Phys. **A231**, 266 (1974).
[15] W. Dunnweber, E. R. Cosman, E. Grosse, W. R. Ering, and P. Von Brentano, Nucl. Phys. **A247**, 251 (1975).
[16] G. J. Igo, P. D. Barnes, E. R. Flynn, and D. D. Armstrong, Phys. Rev. **177**, 1831 (1969).
[17] R. Tickle and W. S. Gray, Nucl. Phys. **A247**, 187 (1975).
[18] G. Igo, E. R. Flynn, B. J. Dropeski, and P. D. Barnes, Phys. Rev. C **3**, 349 (1971).
[19] E. R. Flynn, G. Igo, P. D. Barnes, D. Kovar, and R. Broglia, Phys. Rev. C **3**, 2371 (1971).
[20] G. Audi and A. H. Wapstra, Nucl. Phys. **A595**, 409 (1995).
[21] N. B. Gove and M. J. Martin, Nucl. Data, Sect. A **10**, 206 (1971).
[22] A. H. Wapstra, G. J. Nijgh, and J. Van Lieshout, *Nuclear Spectroscopy Tables* (North Holland, Amsterdam, 1959).
[23] S. Raman and N. B. Gove, Phys. Rev. C **7**, 1995 (1973).
[24] M. J. Martin, Nucl. Data Sheets **63**, 723 (1991).
[25] A. De Shalit and I. Talmi, *Nuclear Shell Theory* (Academic, New York, 1963).
[26] E. Browne, Nucl. Data Sheets **65**, 209 (1992).
[27] T. Lönroth, University of Jjväskylä Departement of Physics, Research Report No. 4/1981, 1981 (unpublished).
[28] E. Caurier (private communication).
[29] G. H. Herling and T. T. S. Kuo, Nucl. Phys. **A181**, 113 (1972).
[30] C. Ellegard, R. P. Barnes, and E. C. Flynn, Nucl. Phys. **A259**, 435 (1976).
[31] E. K. Warburton and B. A. Brown, Phys. Rev. C **43**, 602 (1991).